Acid-Degradable Particles for Protein-Based Vaccines: Enhanced Survival Rate for Tumor-Challenged Mice Using Ovalbumin Model

Stephany M. Standley,[†,‡] Young Jik Kwon,[†,‡] Niren Murthy,[†,‡,§] Jun Kunisawa,[∥] Nilabh Shastri,[∥] Steven J. Guillaudeu,[†,‡] Lana Lau,[‡] and Jean M. J. Fréchet*[,†,‡,§]

Center for New Directions in Organic Synthesis and Departments of Chemistry and Molecular and Cellular Biology, University of California, Berkeley, California 94720-1460, and Materials Sciences Division, Lawrence Berkeley National Laboratory, Berkeley, California 94720. Received February 22, 2004; Revised Manuscript Received September 12, 2004

Acid-degradable protein-loaded polymer particles show promise for antigen-based vaccines due to their ability to activate cytotoxic T lymphocytes (CTLs) in vitro. Protein loadings and cytotoxic T lymphocyte activation efficiencies have now been enhanced through novel delivery vehicle designs. In particular, the use of a more hydrophilic acid-degradable cross-linker leads to increased water dispersibility and increased protein loading efficiency for the particles. A 2.5-fold increase in protein encapsulation allows the delivery of more protein antigen to antigen presenting cells (APCs) leading to a 20-fold rise in antigen presentation levels. The mechanism by which APCs internalize these particles was explored using the phagocytosis inhibitor, cytochalasin B. In addition, preliminary in vivo experiments were conducted to investigate the ability of the protein-loaded particles to provide immunity against tumors in mice, and an enhanced survival rate over the use of protein alone was observed, indicating that this vaccine delivery strategy has great practical potential.

INTRODUCTION

Traditional vaccine strategies have been ineffective at generating vaccines against diseases such as AIDS and hepatitis C, largely due to the high toxicity of the associated live attenuated viruses (*1*). Therefore, new vaccine strategies based on protein antigens are being investigated and have considerable promise due to their low toxicity and widespread applicability (*2*). Protein antigens have been identified for a number of different diseases, such as prostatic acid phosphatase for prostate cancer and gp120 and Tat for HIV, but the effectiveness of each of these would require the development of a more effectual vaccination strategy (*3*, *4*). Efficient protein-based vaccines must be able to activate CTLs, which play a central role in combating viral infections and tumors and generating immunity (*5*, *6*).

A key step in activating CTLs is the delivery of antigens into the cytoplasm of professional APCs, which process these cytoplasmic proteins by degrading them into peptides that are then assembled with major histocompatibility complex (MHC) class I molecules. These MHC class I peptide complexes are transported to the cell surface where they are recognized by antigen specific CTLs, which then become activated and primed to recognize and kill cells that have been infected with that particular antigen.

Therefore, a major challenge in generating this CTL response is to create a vaccine system that can efficiently deliver proteins into the cytoplasm of APCs in order to induce protective immunity against a specific disease. A delivery system is needed because exogenous antigens, proteins not synthesized in the cytoplasm, cannot efficiently reach the cytoplasm of APCs when administered alone as a vaccine because they are taken up through endocytosis and are sequestered and degraded in endosomes or lysosomes of the cell (*7*).

One class of protein delivery systems that is able to introduce exogenous proteins into the cytoplasm of APCs and has shown potential in vaccine research is polymer particles. One advantage of using particles as delivery vehicles is that they can be easily targeted to professional APCs by adjusting their size since it is known that APCs phagocytose particles that are 0.5−3 μm in diameter and cross-linked polymer beads of this size range have been shown to successfully encapsulate proteins (8-11). In theory, these particles could deliver a variety of protein antigens making this technology applicable to many diseases. In addition, encapsulation of proteins inside of the particles protects them from inactivation and unfavorable immune reactions that may occur during delivery.

Antigens associated with particles, such as proteins adsorbed onto polycaprolactone or polystyrene beads, as well as proteins covalently linked to the surface of iron oxide beads, have been shown to present peptides via the MHC class I pathway (*12*, *13*). Also, proteins encapsulated inside poly(lactide-*co*-glycolide) particles have been used to activate CTLs (*14*). These particle-based systems have demonstrated the validity of this method of protein delivery as a useful vaccination strategy. They were thought to weakly disrupt endosomes of APCs after internalization, which allowed a fraction of the protein to be delivered to the cytoplasm. However, while these particles were capable of being taken up by APCs, there

* To whom all correspondence should be addressed. Fax (510) 643-3079. E-mail: frechet@cchem.berkeley.edu.

† Center for New Directions in Organic Synthesis, University of California.

‡ Department of Chemistry, University of California.

§ Material Sciences Division, Lawrence Berkeley National Laboratory.

∥ Department of Molecular and Cellular Biology, University of California.

10.1021/bc049956f CCC: $27.50
Published on Web 10/22/2004

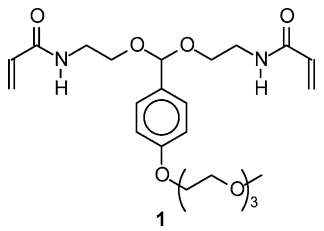

Figure 1. Acid-degradable cross-linker.

was no well-defined mechanism for the transfer of protein from endosomal compartments to the cytoplasm.

To improve upon the cytoplasmic delivery using polymer-based systems, we have reported previously a particle system that was designed to be strongly endosomal disruptive (*15*, *16*). These particles release encapsulated protein in a pH-dependent manner. They are stable at the physiological pH of 7.4 but degrade quickly in the pH 5.0 environment of endosomes, freeing the protein. The rationale for this design, known as the colloid osmotic mechanism (*7*, *17*), is to generate a quick degradation of the particles into many molecules, thus increasing the osmotic pressure within the endosome, leading to a rapid influx of water across the membrane resulting in its disruption. Rupture of the endosomal compartment affords the viral antigen an outlet to the cytoplasm of the cell while also circumventing the possible degradation of the protein by hydrolytic enzymes present in the mildly acidic endosome.

The acid-sensitive protein-loaded particles were synthesized by copolymerizing an acid-degradable cross-linker, **1** (Figure 1) and acrylamide in the presence of a protein using an inverse emulsion polymerization technique. Preliminary experiments have demonstrated that these particles were nontoxic and were capable of MHC class I presentation and CTL activation in vitro, which was determined by the LacZ assay (*16*). Although this system showed promise for applications in vaccine development, this new strategy had not been optimized or evaluated using in vivo experiments.

In this report the protein-loading capacity and enhanced water dispersibility of the particle system are investigated. In addition, we present in vitro studies evaluating the CTL activation levels of the optimized particles and discuss the mechanism by which the particles are internalized by APCs. Finally, preliminary in vivo experiments testing the ability of the protein delivery vehicle to provide a protective immunity against tumors using an ovalbumin model are presented.

EXPERIMENTAL PROCEDURES

General Procedures and Materials. Tetrahydrofuran was distilled under a nitrogen atmosphere from Na/benzophenone immediately prior to use. *p*-Toluenesulfonic acid was dehydrated and then recrystallized from toluene. *N*-(2-Hydroxyethyl)-2,2,2-trifluoroacetamide and acryloyl chloride were freshly distilled before each use. Combined organic layers after extractions were dried over anhydrous $MgSO_4$. Solvents were removed under reduced pressure using a rotary evaporator. Merck Kieselgel plates coated with silica gel 60 F_{254} were used for thin-layer chromatography, and compounds were visualized by UV activity. Flash column chromatography was done with Merck Kieselgel 60 silica gel (230−400 Mesh). Mice were purchased from Jackson Laboratory, and cells were purchased from the ATCC. The SIINFEKL peptide was purchased from the Synpep Corporation. The antibody 25.D1-16 was produced from the hybridoma cells generously provided by Dr. Ronald Germain of NIAID, and the goat anti-mouse antibody labeled with R-phycoethrin (PE) was purchased from Pharmingen.

Characterization. ^{1}H NMR spectra were recorded at 300 or 400 MHz, and ^{13}C spectra were recorded at 100 MHz. NMR chemical shifts are reported in ppm relative to tetramethylsilane (TMS) and are calibrated against residual solvent peaks: $CDCl_3$ (δ 7.26, δ 77.23) or DMSO-d_6 (δ 2.49, δ 39.51). All coupling constants are reported in Hz. High-resolution fast atom bombardment mass spectrometry (FAB-HRMS) experiments were performed at the UC−Berkeley mass spectrometry facility. FT-IR spectroscopic analyses were performed using a thin film cast from $CHCl_3$ on a reflective mirror surface. Elemental analyses were performed by M-H-W Laboratories or at the UC−Berkeley Analytical Laboratory.

***N,N′*-Diacryloyl-bis(2-aminoethoxy)-[4-(1,4,7,10-tetraoxaundecyl)phenyl]methane (1).** This compound was prepared according to literature procedure (*16*).

1-Chloro-3,6,9,12-tetraoxatridecane (3). This compound was prepared according to the reaction conditions reported by Schafheute et. al. used to prepare 1-chloro-3,6,9,12,15-pentaoxahexadecane (*18*). This procedure was modified by using dichloroethyl ether as the dichloride compound. The product was isolated by short path distillation (106 °C/2 mmHg). IR (cm^{-1}): 2875 (s), 1149 (s). ^{1}H NMR (300 MHz, $CDCl_3$): δ 3.38 (s, 3), 3.55 (t, 2, J = 4.6), 3.75 (t, 2, J = 5.9), 3.60−3.67 (m, 12). ^{13}C NMR ($CDCl_3$): δ 42.36, 58.60, 70.11, 70.19, 70.21, 70.24, 70.96, 71.55. Calcd: $[M + H]^+$ ($C_9H_{20}O_4Cl$) m/z = 227.1050. Found FAB-HRMS: $[M + H]^+$ m/z = 227.1045. Anal. Calcd. for $C_9H_{19}O_4$: C, 47.68; H, 8.45. Found: C, 47.83; H, 8.62.

***p*-(1,4,7,10,13-Pentaoxatetradecyl)benzaldehyde (4).** Chloride **3** (13.3 g, 58.6 mmol, 1.5 equiv) and *p*-hydroxybenzaldehyde (4.78 g, 39.1 mmol, 1 equiv) were dissolved in dry THF (15 mL). K_2CO_3 (5.4 g, 39.1 mmol, 1 equiv) was added followed by 18-crown-6 (103 mg, 0.39 mmol, 0.01 equiv) and KI (64.9 mg, 0.39 mmol, 0.01 equiv). The reaction mixture was stirred at reflux for 48 h. The resulting mixture was cooled to room temperature, and water (150 mL) was added. The product was extracted with three 150 mL portions of ethyl acetate, and the combined organic layers were dried and concentrated. The oil was loaded onto a silica gel column and eluted with a 1:1 mixture of ethyl acetate/hexane to afford 11.8 g (97%) of **4** as a clear oil. IR (cm^{-1}): 1693 (s), 1132 (s). ^{1}H NMR (300 MHz, $CDCl_3$): δ 3.33 (s, 3), 3.50 (t, 2, J = 4.5), 3.72−3.58 (m, 10), 3.86 (t, 2, J = 4.8), 4.18 (t, 2, J = 4.8), 6.99 (d, 2, J = 8.7), 7.79 (d, 2, J = 8.6), 9.80 (s, 1). ^{13}C NMR ($CDCl_3$): δ 58.82, 67.59, 69.26, 70.32, 70.41, 70.43, 70.69, 71.73, 114.70, 129.84, 131.74, 163.68, 190.59. Calcd: $[M + H]^+$ ($C_{16}H_{25}O_6$) m/z = 313.1651. Found FAB-HRMS: $[M + H]^+$ m/z = 313.1643.

***N,N′*-Bis(trifluoroacetyl)-bis(2-aminoethoxy)-[4-(1,4,7,10,13-pentaoxatetradecyl)phenyl]methane (5).** Aldehyde **4** (6.65 g, 21.3 mmol, 1 equiv) and *N*-(2-hydroxyethyl)-2,2,2-trifluoroacetamide (25.4 g, 161.8 mmol, 7.6 equiv) were dissolved in dry THF (40 mL). *p*-Toluenesulfonic acid (586 mg, 3.4 mmol, 0.16 equiv) and 5 Å molecular sieves (52 g) were added. The reaction mixture was stirred overnight and then quenched with triethylamine (3.8 mL, 27.7 mmol, 1.3 equiv). The reaction mixture was filtered, and water (150 mL) was added to the filtrate. The product was extracted with five 150 mL portions of ethyl acetate, and the solvent was evaporated. To remove the excess alcohol, benzoyl chloride (16.3 mL, 140.4 mmol, 1 equiv), triethylamine (40.0 mL, 280.8 mmol, 2 equiv), and dry THF (100 mL) were

added. The reaction mixture was stirred at room temperature for 1 h. Water (250 mL) was added and the product was extracted with five 250 mL portions of ethyl acetate, and the solvent was evaporated. The remaining oil was loaded onto a silica gel column and eluted with a 3:7 mixture of ethyl acetate/hexane, followed by a 4:1 mixture of ethyl acetate/hexane to afford 10.4 g (82%) of **5** as a white solid. MP: 74.6−75.0 °C. IR (cm^{-1}): 3292 (br), 1701 (s), 1560 (m), 1209 (s), 1178 (s). ^1H NMR (400 MHz, DMSO-d_6): δ 3.21 (s, 3), 3.34−3.41 (m, 6), 3.46−3.58 (m, 14), 3.72 (t, 2, $J = 4.6$), 4.07 (t, 2, $J = 4.6$), 5.52 (s, 1), 6.91 (d, 2, $J = 8.4$), 7.29 (d, 2, $J = 8.4$), 9.53 (t, 2, $J = 5.6$). ^{13}C NMR (DMSO-d_6): δ 39.22, 58.01, 62.56, 67.12, 68.89, 69.56, 69.76, 69.81, 69.91, 71.26, 100.54, 113.92, 115.19 (q, $J = 288$), 127.72, 130.25, 156.38 (q, $J = 36$), 158.51. Calcd: $[M]^+$ ($C_{24}H_{34}F_6N_2O_9$) $m/z = 608.2168$. Found FAB-HRMS: $[M]^+$ $m/z = 608.2153$. Anal. Calcd. for $C_{24}H_{34}F_6N_2O_9$: C, 47.37; H, 5.63; N, 4.60. Found: C, 47.20; H, 5.84; N, 4.54.

***N,N′*-Diacryloyl-bis(2-aminoethoxy)-[4-(1,4,7,10,-13-pentaoxatetradecyl)phenyl]methane (2).** Compound **5** (0.40 g, 0.66 mmol, 1 equiv) and 6 M NaOH (2.8 mL) were added to dioxane (1.8 mL), and the reaction mixture was stirred at room temperature for 3.5 h. Upon complete removal of the acetamide groups, as determined by TLC using ninhydrin staining, the reaction mixture was cooled to 0 °C and triethylamine (0.6 mL) was added. Acryloyl chloride (1.1 mL, 14 mmol, 21 equiv) and triethylamine (5.6 mL, 40.0 mmol, 61 equiv) were added in small alternating portions while periodically monitoring the pH to maintain it above 7. A 10% K_2CO_3 in water solution (40 mL) was added, and the reaction was stirred for 10 min before extracting the product with six 40 mL portions of ethyl acetate. The organic layers were dried and concentrated to afford a yellow oil. The crude product was purified by column chromatography and eluted with a 2:1 mixture of ethyl acetate/hexane, followed by ethyl acetate, and a 1:9 mixture of methanol/ethyl acetate to afford 0.20 g (58%) of **2** as a white solid. MP: 62.0−63.0 °C. IR (cm^{-1}): 3302 (br), 1657 (s), 1541 (m), 1102 (s). ^1H NMR (300 MHz, DMSO-d_6): δ 3.21 (s, 3), 3.29 (t, 2, $J = 4.5$), 3.39−3.55 (m, 18), 3.72 (t, 2, $J = 4.6$), 4.07 (t, 2, $J = 4.6$), 5.49 (s, 1), 5.56 (dd, 2, $J = 10$, $J = 2$), 6.10 (dd, 2, $J = 17$, $J = 2$), 6.30 (dd, 2, $J = 17$, $J = 10$), 6.90 (d, 2, $J = 8.6$), 7.32 (d, 2, $J = 8.6$), 8.20 (t, 2, $J = 5.5$). ^{13}C NMR (DMSO-d_6): δ 38.67, 58.01, 63.77, 67.07, 68.88, 69.54, 69.74, 69.78, 69.89, 71.24, 100.80, 113.88, 125.06, 127.83, 130.60, 131.67, 131.87, 158.42, 164.68. Calcd: $[M + Li]^+$ ($C_{26}H_{40}N_2O_9Li$) $m/z = 531.2893$. Found FAB-HRMS: $[M + Li]^+$ $m/z = 531.2883$. Anal. Calcd. for $C_{26}H_{40}N_2O_9$: C, 59.53; H, 7.69; N, 5.34. Found: C, 59.19; H, 7.63; N, 5.04.

Inverse Emulsion Polymerization. To generate protein-loaded particles, an inverse emulsion polymerization technique was used. The organic phase consisted of hexane (5 mL) and 150 mg of surfactants. A 3:1 weight ratio of Span 80 (sorbitan monooleate) and Tween 80 (poly(ethylene glycol)−sorbitan monooleate) was used. The oxygen dissolved in the organic phase was removed by sparging with nitrogen for 10 min. The aqueous phase consisted of acrylamide and cross-linker (250 mg combined in a range of ratios) dissolved in 300 mM sodium phosphate-buffered water (pH 8, 500 μL). The oxygen dissolved in the aqueous phase was removed by purging with nitrogen for 1 min. Free radical initiator, potassium peroxodisulfate (12 mg), and ovalbumin (labeled with cascade blue dye or unlabeled) were added to the aqueous phase and then emulsified with the organic phase by sonicating for 30 s. Polymerization was initiated by the addition of *N,N,N′,N′*-tetramethylethylenediamine (TMEDA) and stirred for 10 min at room temperature. The mixture was centrifuged at 2800 rpm for 10 min, and the supernatant was decanted. The particles were washed with two 20 mL portions of hexane, followed by four 20 mL portions of acetone, and finally centrifuged. The solvent was decanted, and the purified particles were dried in vacuo overnight.

Nondegradable particles were prepared using the method described above using *N,N′*-methylene-bis-acrylamide as the cross-linker. The mole percent of cross-linker and total weight of monomer and cross-linker combined were the same as above.

Scanning Electron Microscopy. The particles were dried in vacuo to remove residual water, sputter-coated with a 20 nm gold layer, and viewed in a scanning electron microscope (WDX ISI-ds130C, Microspec Corporation, Inc.). Photographs were taken at 15 kV.

Protein Encapsulation Measurements. A small amount of each particle sample (2 mg) containing ovalbumin labeled with cascade blue was dispersed in 300 mM sodium phosphate-buffered water (pH 8, 500 μL). The samples were then centrifuged for 5 min, and the supernatant was removed. The pellet was then redispersed into 300 mM sodium acetate buffered water (pH 1.6, 500 μL). Once completely hydrolyzed, the fluorescence emission of the aqueous solution was measured at 405 nm with an excitation at 355 nm. The unknown protein concentration of each particle sample was calculated by fitting the emission to a calibration curve made from known concentrations of ovalbumin labeled with cascade blue. The background emission of the buffer was measured and subtracted from all of the readings. Each sample was done in triplicate.

The protein determination of the nondegradable particles was performed differently since they do not degrade in acidic conditions. The samples were weighed and washed in a pH 8 buffer. The solid was then redispersed into 6 M NaOH to hydrolyze the protein−cascade blue into smaller pieces that could diffuse out of the particles. After 1 day, the solid was removed by centrifugation and the fluorescence emission of the aqueous solution was measured at 405 nm with an excitation at 355 nm. The unknown protein concentration of each microparticle sample was calculated by fitting the emission to a calibration curve made from known concentrations of ovalbumin−cascade blue that had been dissolved in 6 M NaOH for the same period of time. Each sample was done in triplicate, and degradable particles were also analyzed at the same time in this fashion for direct comparison. Although the amount of protein measured for the degradable samples using this method was higher than found for the method above, a relative comparison between the samples was performed.

Class I Antigen Presentation Assay. The class I antigen presentation assay (LacZ assay) was performed using the OVA-derived SIINFEKL peptide/K^b-specific B3Z T cell hybridoma and RAW 309.1 CR antigen presenting cells. RAW cells were plated at 5×10^4 cells per well in a 96-well plate and allowed to grow overnight. Ovalbumin loaded particles were dispersed in DMEM medium (5 mg/mL) and sonicated for 5 min. An appropriate amount of the particle stock solution was added to the cells, in a 100 μL volume. The RAW cells were incubated with the particles for 6 h at 37 °C and then washed several times with DMEM medium. B3Z cells (1×10^5) were added to the RAW cells, and the two cell lines were incubated together for 16 h in RPMI media at 37 °C. LacZ activity was measured as the absorbance at 595 nm of the cleavage product of chlorophenol red-β-D-

galactopyranoside. All samples were performed in triplicate.

For each antigen presentation assay performed, a standard peptide curve was prepared by incubating the RAW cells with a series of SIINFEKL concentrations alongside the particle samples. The absorbance at 595 nm was plotted against the log of the peptide concentration. The resulting curve was sigmoidal, but only the optimal concentrations were used for the linear standard so high and low concentrations were deleted. The trendline equation was then used to quantify the amount of peptide presented using the absorbance values.

Cytochalasin B Assay. To inhibit phagocytosis, RAW cells were incubated in a 17 μM solution of cytochalasin B in DMEM 2 h before the particle samples were added. Identical particle samples were added to both the inhibited and uninhibited groups of cells in triplicate. The remainder of the experiment was the same as described above for the class I antigen presentation assay.

In Vivo Tumor Protection Experiment. Experiments were performed with female C57BL/6 mice and all immunizations were administered by subcutaneous injections using 26 gauge needles. There were three groups (15 mice per group): control mice injected with saline (200 μL); mice injected with free ovalbumin in saline (50 μg in 200 μL); and mice injected with ovalbumin encapsulated in particles (Sample D) dispersed in saline (1.13 mg particles, corresponds to 50 μg ovalbumin, in 200 μL). A second identical immunization was delivered 2 weeks after the first. Then 10 days after the second immunization, tumors were established by administering an injection of 1×10^6 EG7-OVA tumor cells in 100 μL saline into the shaved left flank of each mouse. One week prior to injection, the EG7 cells were stained with the anti-SIINFEKL/K^b monoclonal antibody 25.D1-16 and the secondary goat anti-mouse antibody labeled with R-phycoethrin (PE). Then highly ovalbumin-expressing cells were collected using flourescence-activated cell sorting (FACS) and proliferated. After injection, the tumor growth was monitored by measuring two perpendicular axes using digital calipers. Tumor volume was then calculated using the equation, volume $= 0.5 \times$ length $\times$ width^2, with the length being the longest diameter and the width being the shortest diameter of the two perpendicular measurements. Once the tumor reached 1.5 cm in average diameter, the mouse was removed from the experiment and euthanized according to guidelines set by the UC−Berkeley Animal Care and Use Committee. Mice were also removed if they showed other signs of pain or distress such as a lack of cleaning, eating, or mobility. A log rank test was used to determine *p*-values. A *p*-value of 0.05 or less was considered to be statistically significant.

RESULTS AND DISCUSSION

Controlling the Hydrophilicity of the Cross-Linker. The dispersibility of particles made with cross-linker **1**, while sufficient for proof-of-concept experiments, required further improvement, as the particles it afforded as a white powder could be suspended in an aqueous solution, but they readily aggregated and formed a precipitate. For practical application as a vaccine, the material should be uniformly dispersed in solution, enabling it to be used by injection. Covering the particle surface with a long hydrophilic oligoethylene glycol layer would be expected to enhance the colloidal properties of the particles in water due to greater hydration and steric stabilization afforded by the layer (*19*−*21*). However, the use of high molecular weight poly(ethylene glycol) chains was not pursued since it has been shown that a 5 kDa poly(ethylene glycol) surface on poly(lactic-*co*-glycolic acid) particles diminished the recognition of particles by phagocytic cells, and this would clearly be detrimental in our target application (*20*). To balance the need for enhanced hydrophilicity and the requirements of inverse microemulsion polymerization (*16*), we prepared cross-linker **2** in which the solubilizing group is extended by one ethylene oxide unit over that of our earlier cross-linker **1**.

Scheme 1. Synthesis of Cross-Linker

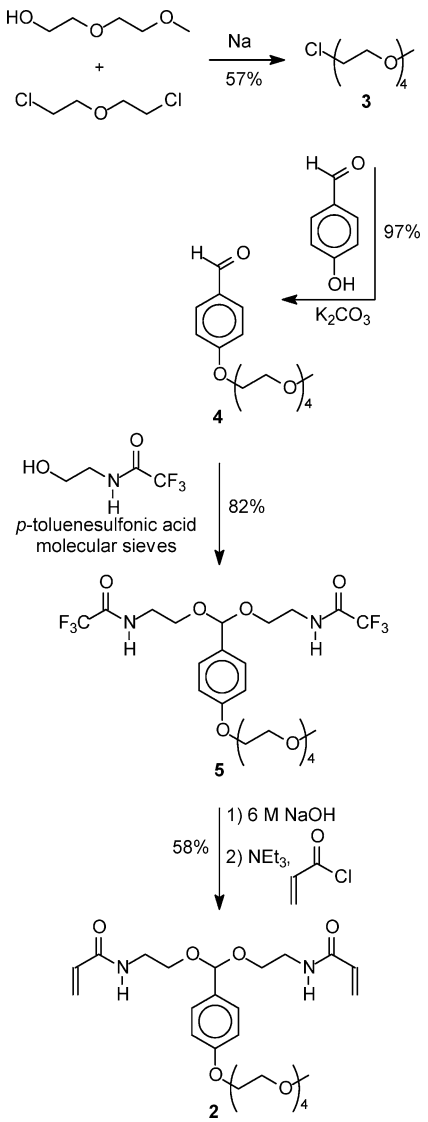

This target molecule **2** was prepared in four steps as shown in Scheme 1. 1-Chloro-3,6,9,12-tetraoxatridecane, **3**, was prepared and coupled to *p*-hydroxybenzaldehyde and K_2CO_3 to afford **4** in 97% yield. Intermediate **5** was synthesized in 82% yield by reaction of **4** with *N*-(2-hydroxyethyl)-2,2,2-trifluoroacetamide in the presence of a catalytic amount of *p*-toluenesulfonic acid and a drying agent to shift the equilibrium toward the acetal product. To install the polymerizable handles, the primary amine groups of **5** were deprotected with 6 M NaOH and coupled to acryloyl chloride in dioxane using biphasic conditions, affording **2** in 58% yield. Triethylamine was added in the final step to quench any HCl byproduct in order to avoid any possible and untimely degradation of the acid labile acetal.

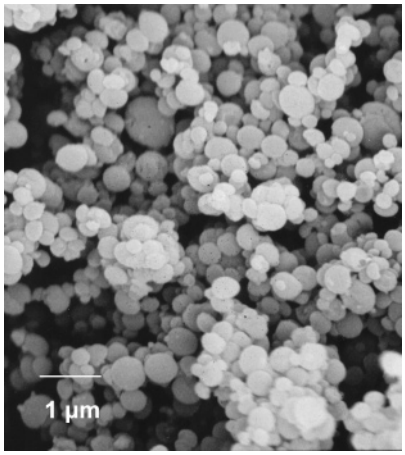

Figure 2. SEM image of particles prepared with cross-linker 2.

Inverse Emulsion Polymerization with Cross-Linker 2. Cross-linked protein-loaded particles were synthesized using **2** and acrylamide as the monomers in an inverse microemulsion polymerization process (*16*, *22*). First, **2** and acrylamide were dissolved in buffered water, and ovalbumin and the polymerization initiator, potassium peroxodisulfate, were then added. The aqueous phase was dispersed into an organic phase, which consisted of a 3:1 blend of Span 80 and Tween 80 surfactants in hexane. Span 80 and Tween 80 were chosen because they are nonionic and nontoxic. The emulsion was created by sonication and polymerization was initiated upon addition of TMEDA. After polymerization, the particles were isolated by centrifugation, washed, and dried to remove residual hexane and surfactants. The particle size ranged from 250 to 500 nm in diameter, as determined by Figure 2, and we observed that the particles were readily dispersible in water unlike particles synthesized with the less hydrophilic cross-linker **1**.

Protein Loading Studies. Increasing the amount of protein encapsulated in the particles was an important step in developing an effective and better controlled delivery system. Ideally, the amount of protein delivered to an APC per particle would be large enough to produce efficient MHC class I presentation. This is especially important for in vivo experiments where a smaller number of particles per cell would be taken up as compared to tissue culture. In initial studies with cross-linker **1** (*16*), it was noted that the protein loading did not change with the degree of cross-linking. Therefore, protein loading studies were carried out using a fixed amount of cross-linker **1** (12.8%) and acrylamide in the polymerization mixture, varying only the concentration of ovalbumin labeled with cascade blue. Following inverse microemulsion polymerization, the amount of protein encapsulated was determined for each sample by hydrolyzing the particles in acidic conditions until the solution became completely clear and then measuring the fluorescence of the released ovalbumin in solution.

Protein loading increased with initial ovalbumin concentration in the polymerization mixture as shown in Table 1. For example, when the initial amount of protein in the polymerization was tripled from 5.4 mg to 16.8 mg, the amount of ovalbumin encapsulated doubled from 9.5 μg/mg to 22.0 μg/mg as illustrated by samples A (*16*) and B in Table 1. Also, when the initial amount was 33.2 mg, the final ovalbumin loading increased 6-fold from 9.5 to 62.6 μg/mg as shown in sample C. The appearance and stability of the particles remained the same even though more protein had been encapsulated. The maximum ovalbumin encapsulation achieved with this system using cross-linker **1** was 62.6 μg/mg particles for sample C. The use of higher initial protein concentrations in reaction mixtures involving this set of monomers and polymerization conditions resulted in a large amount of aggregation and precipitation during the polymerization.

Table 1. Particle Samples with Increased Protein Loading

sample	cross-linker	initial amount of cascade blue-labeled ovalbumin (mg)	encapsulated ovalbumin/particles (μg/mg)
A	1	5.4	9.5
B	1	16.8	22.0
C	1	33.2	62.6
D	2	5.2	44.3
E	2	33.0	135.6
F	2	45.6	154.8

The same experiments were performed using the new, more hydrophilic, cross-linker **2** with the same mole percent of cross-linker (12.8%), keeping the total amount of monomers (acrylamide and **2**) constant. The concentration of ovalbumin labeled with cascade blue in the initial polymerization mixture was varied as shown in Table 1. Unexpectedly, higher protein encapsulation efficiencies were achieved using the more hydrophilic **2**. This increase in efficiency may be due to increased stabilization of the particles and protein in the emulsion or aqueous solution causing less protein aggregation and precipitation. The protein encapsulation efficiency of particles made with **2** was over twice that of particles made with **1**. For example, when 33 mg of ovalbumin was added to the initial mixture, the loading of particles made with **1** was 62.6 μg ovalbumin/mg particles (sample C), whereas the loading of particles made with **2** was 135.6 μg protein/mg particles (sample E). The maximum protein encapsulation obtained with cross-linker **2** was 154.8 μg ovalbumin/mg particles in sample F. Therefore, our goals of increasing the hydrophilicity of the particles while achieving better control over their protein content were met with the development and application of cross-linker **2**.

Antigen Presentation Experiments with Highly Loaded Particles. LacZ antigen presentation assays, developed by Karttunen et al., were performed to determine if the increased encapsulation of protein in the acid-degradable particles resulted in enhanced cytoplasmic delivery of protein to APCs, leading to higher MHC class I presentation levels and CTL activation (*23*). To demonstrate CTL activation, the particles were first incubated at various concentrations with the antigen presentation cell line, RAW 309.1 CR, for 6 h. After removal of extracellular particles, the APCs were incubated with ovalbumin specific B3Z cells. These B3Z cells are CTLs engineered to secrete β-galactosidase after binding to the ovalbumin-derived SIINFEKL peptide in a MHC class I (K^b)-restricted manner. This allows T cell activation to be quantified by β-galactosidase activity. Higher β-galactosidase activity, quantified by absorbance measurements at 595 nm due to release of a dye, infers greater antigen presentation and CTL activation levels. The measured absorbance values at 595 nm can then be converted into the corresponding concentration of SIINFEKL peptide presented using a standard peptide curve.

An antigen presentation assay was run testing samples A, B, C, and E since they displayed a range of protein loadings. Figure 3 illustrates that higher ovalbumin loadings lead to greater antigen presentation levels as

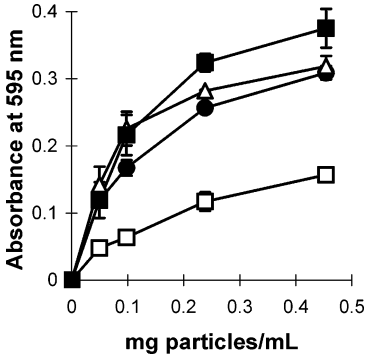

Figure 3. Antigen presentation assay testing particles with varied protein loadings. Sample A (□); sample B (●); sample C (△); sample E (■).

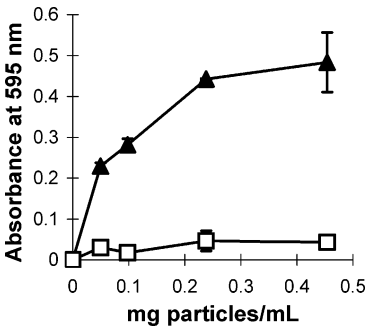

Figure 4. Effect of degradability on antigen presentation. Degradable (▲); nondegradable (□).

indicated by higher β-galactosidase activity. Also, increasing sample concentration leads to greater antigen presentation levels. These trends are likely due to the rise in the amount of ovalbumin delivered to the cytoplasm of the APCs, leading to more SIINFEKL peptide presentation. For example, at a sample concentration of 0.45 mg particles/mL, after conversion of absorbance values to presented peptide concentration, sample E shows a 20-fold enhancement over sample A which we reported previously in our proof-of-concept system (*16*).

To determine if the acid-degradable characteristic of the particles enhanced MHC class I presentation, a nondegradable ovalbumin-loaded particle sample was synthesized using *N*,*N*′-methylene-bis-acrylamide as the stable cross-linker. An antigen presentation study was then performed comparing nondegradable and degradable particles with similar protein content. Figure 4 clearly demonstrates that the degradable particles enhance MHC class I presentation, suggesting that the hydrolysis of the cross-linker and release of small molecules in the lysosome may help to destabilize the membrane resulting in the transport of protein into the cytoplasm for processing.

Phagocytosis-Mediated Antigen Delivery into MHC Class I Presentation. To help determine if the particles enter APCs through the process of phagocytosis, antigen presentation assays were performed in the presence of a phagocytosis inhibitor, cytochalasin B (*13*). Cytochalasin B inhibits phagocytosis by preventing actin polymerization and the interaction of actin filaments. Figure 5i shows that the antigen presentation levels for the cells incubated with the inhibitor are greatly reduced as compared to the cells that were not. For example, at the highest particle concentration, the calculated concentration of presented peptide for cells incubated with the inhibitor is only 30% of the peptide presented as calculated for the cells incubated without cytochalasin B. This finding is consistent with a process in which the particles undergo phagocytosis. Another key point is that the peptide presentation levels of the cells incubated without cytochalasin B are very close to the concentration of presented peptide at saturation (Figure 5ii). The saturation concentration is determined from the standard peptide curve, which is prepared by adding free SIINFEKL peptide to the RAW cells in various concentrations. This free peptide is not delivered to the cytoplasm of the RAW cells, but instead directly binds to MHC class I molecules that are on the surface of the cells. These SIINFEKL complexes can also activate the B3Z cells. The concentration of free SIINFEKL at which the absorbance at 595 nm levels off is considered to represent the saturation concentration of presented peptide, which was 2 nM in this experiment (Figure 5ii). For the particle sample, at 0.45 mg particles/mL the concentration of peptide presented without the phagocytosis inhibitor is 1.7 nM of peptide (Figure 5i), which is near the saturation level. This study suggests that this acid-sensitive particle system is very efficient for in vitro delivery of the protein antigen into the MHC class I presentation pathway.

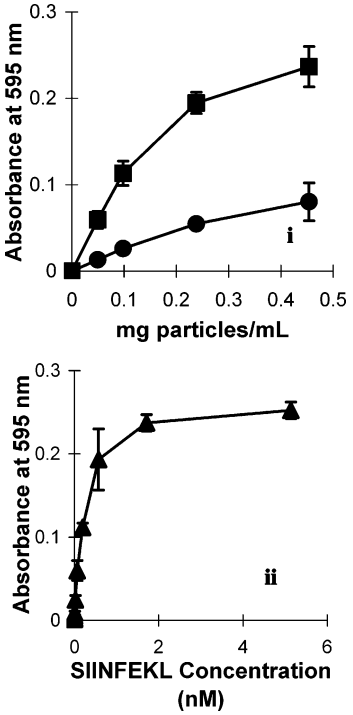

Figure 5. (i) Antigen presentation assay with phagocytosis inhibitor. Sample D (■); sample D with cytochalasin B (●). (ii) Antigen presentation assay of SIINFEKL peptide.

In Vivo Tumor Protection. To assess the ability of the acid-degradable protein-loaded particles to deliver protein to the cytoplasm of APCs and activate CTLs and provide a protective immunity in vivo, a preliminary tumor protection experiment was performed using the EG7 tumor model (*24*, *25*). EG7 is a derivative of the thymoma EL4, which was transfected with the ovalbumin gene, making it a target cell for CTLs activated against ovalbumin. Sample D was chosen for this experiment because it had the best dispersibility of all of the samples in Table 1, an important consideration for the study since the particles had to be suspended in saline and injected into animals. Samples E and F, although also prepared with cross-linker **2**, were somewhat more difficult to suspend than Sample D, most likely due to a degree of particle aggregation as a result of higher ovalbumin content.

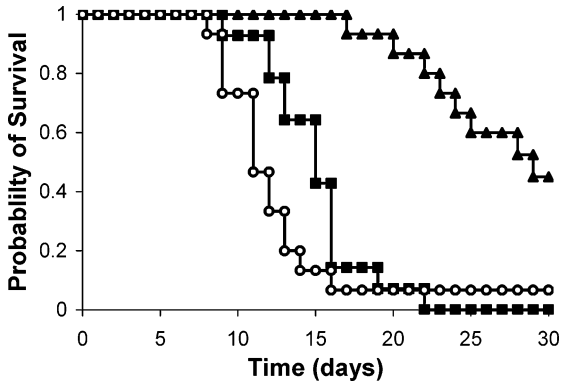

Figure 6. Kaplan−Meier survival plot. Saline (○); free ovalbumin (■); ovalbumin in particles (▲).

The experiment involved three groups of animals as follows: mice immunized with free ovalbumin, mice immunized with an equal amount of ovalbumin encapsulated in the particles (Sample D), and a control group receiving only saline. Each mouse received two subcutaneous immunizations that were 2 weeks apart. Ten days after the final immunization, EG7 tumor cells that had been previously sorted into a set of highly ovalbumin expressing cells were injected subcutaneously into each mouse, and tumor growth was then monitored, with Day 1 being the first day of tumor establishment. Tumors were visible on almost all of the mice in the saline and free ovalbumin groups 7 days after the EG7 injection, whereas 13 out of 15 mice in the particle group did not show any visible tumors until Day 16. In general, tumor growth in the saline control group occurred early in the experiment and was very rapid, resulting in the removal of all but 1 mouse by Day 16. The free ovalbumin group also demonstrated tumor growth early in the experiment but at a slower rate resulting in the removal of all mice from the study by Day 21. For the mice receiving particles, EG7 tumors were not observed until midway through the experiment, and the growth was slower in comparison to the other groups. At the completion of the study, Day 30, five mice in the particle group had yet to be removed from the experiment, although they did have tumors. The trends seen in tumor growth also correlated with the survival rates. This can be seen in the Kaplan−Meier survival plot (Figure 6). The slope of the saline and free ovalbumin series is much steeper than the particle series. The mice that received the particles had a survival rate of 100% after 17 days versus approximately 14% and 7% for the free ovalbumin and saline groups, respectively. The probability of survival eventually dropped to 0% for the free ovalbumin mice by Day 22 while the saline group remained at 7% while the particle group only fell to 45% by the end of the experiment. There was a statistically significant difference between the particle group and the other two groups (compared to saline $p < 0.0001$; compared to ovalbumin alone $p < 0.00001$), but there was no difference between the ovalbumin and saline groups ($p > 0.1$). These encouraging preliminary results suggest that the particles can stimulate an immune response against EG7 tumor cells that is more effective than ovalbumin alone, indicating that the particles can provide a protective immune response against tumor cells in vivo. Future experiments will seek to improve these results by taking advantage of the synthetic flexibility of the system through incorporation of APC targeting and immunostimulatory groups such as mannose and CpG DNA into the particles (*6*, *26*−*28).* Additional studies will also test samples with varied doses and protein loadings to determine if these variables have the same effect in vivo as they do in vitro.

CONCLUSION

This study confirms that tuning the hydrophilicity of acid-degradable cross-linkers such as **2** can be used to enhance the potential of antigen-loaded particles for the delivery of vaccines. Particles prepared with this cross-linker have higher protein loading efficiencies and better dispersibility in aqueous solution than our earlier proof-of-concept system. The MHC class I presentation levels achieved with these particles are vastly enhanced as a result of their ability to deliver more protein into the cytoplasm of APCs. Experiments involving the addition of cytochalasin B, which significantly reduces MHC class I antigen presentation levels provide support for our assumption of a phagocytosis mechanism for the internalization of these particles. Initial animal studies showed promising results with the demonstration that these acid-sensitive particles can stimulate the immune system against an injected protein resulting in the enhanced rejection of EG7 tumor cells in vivo. This new protein delivery system should find applications in vaccines targeted against viruses and tumors, where the activation of CTLs is required for the generation of immunity.

ACKNOWLEDGMENT

We thank Ann Fischer (UC Berkeley Cell Culture Facility) for help with the cell culture studies and Lindsey Jennings (UC Berkeley Animal Facility) for help with the animal studies. We thank the U.S. Department of Energy (Grant DE-ACO3-76SF00098) for funding the development of biocompatible acid-degradable particles and the National Institute of Health (Grant RO1EB002047) for funding the biological studies. Jun Kunisawa is a Research Fellow of the Japan Society for the Promotion of Science. The Center for New Directions in Organic Synthesis is supported by Bristol-Myers Squibb as the Sponsoring Member and Novartis as a Supporting Member.

LITERATURE CITED

(1) Blower, S. M., Koelle, K., Kirschner, D. E., and Mills, J. (2001) Live attenuated HIV vaccines: predicting the tradeoff between efficacy and safety. *Proc. Natl. Acad. Sci. U.S.A. 98*, 3618−3623.

(2) Berzofsky, J. A., Ahlers, J. D., and Belyakov, I. M. (2001) Strategies for designing and optimizing new generation vaccines. *Nat. Rev. Immunol. 1*, 209−219.

(3) Fong, L., and Engleman, E. G. (2000) Dendritic cells in cancer imunnotherapy. *Annu. Rev. Immunol. 18*, 245−273.

(4) Goldstein, G. (1996) HIV-1 Tat protein as a potential AIDS vaccine. *Nat. Med. 1*, 960−964.

(5) Letvin, N. L., Barouch, D. H., and Montefiori, D. C. (2002) Prospects for vaccine protection against HIV-1 infections and AIDS. *Annu. Rev. Immunol. 20*, 73−99.

(6) Merad, M., Sugie, T., Engleman, E. G., and Fong, L. (2002) In vivo manipulation of dendritic cells to induce therapeutic immunity. *Blood 99*, 1676−1682.

(7) Moore, M. W., Carbone, F. R., and Bevan, M. J. (1988) Introduction of soluble protein into the class I pathway of antigen processing and presentation. *Cell 54*, 777−785.

(8) Seymour, L., Schacht, E., and Duncan, R. (1991) The effect of size of polystyrene particles on their retention within the rat peritoneal compartment, and on their interaction with rat peritoneal macrophages in vitro. *Cell Biol. Int. Rep. 15*, 277−286.

(9) O′Hagan, D. T., Palin, K., Davis, S. S., Artursson, P., and Sjöholm, I. (1989) Microparticles as potentially orally active immunological adjuvants. *Vaccine 7*, 421−424.
(10) Ekman, B., Lofter, C., and Sjöholm, I. (1976) Incorporation of macromolecules in microparticles: preparation and characteristics. *Biochemistry 15*, 5115−5120.
(11) Edman, P., Ekman, B., and Sjöholm, I. (1980) Immobilization of proteins in microspheres of biodegradable polyacryldextran. *J. Pharm. Sci*. *69*, 838−842.
(12) Oh, Y., Harding C. V., and Swanson, J. A. (1997) The efficiency of antigen delivery from macrophage phagosomes into cytoplasm for MHC class I-restricted antigen presentation. *Vaccine 15*, 511−518.
(13) Kovacsovics-Bankowski, M., Clark, K., Benacerraf, B., and Rock K. L. (1993) Efficient major histocompatibility complex class I presentation of exogenous antigen upon phagocytosis by macrophages. *Proc. Natl. Acad. Sci. U.S.A. 90*, 4942−4946.
(14) Moore, A., McGuirk, P., Adams, S., Jones W. C., McGee, J. P., O′Hagan, D. T., and Mills, K. H. G. (1995) Immunization with a soluble recombinant HIV protein entrapped in biodegradable microparticles induces HIV-specific $CD8^+$ cytotoxic T lymphocytes and $CD4^+$ Th1 cells. *Vaccine 13*, 1741−1749.
(15) Murthy, N., Thng, Y. X., Schuck, S., Xu, M., and Fréchet, J. M. J. (2002) A novel strategy for encapsulation and release of proteins: hydrogels and microgels with acid-labile acetal cross-linkers. *J. Am. Chem. Soc*. *124*, 12398−12399.
(16) Murthy, N., Xu, M., Schuck, S., Kunisawa, J., Shastri, N., and Fréchet, J. M. J. (2003) A macromolecular delivery vehicle for protein-based vaccines: acid-degradable protein-loaded microgels. *Proc. Natl. Acad. Sci. U.S.A. 100*, 4995−5000.
(17) Okada, C. Y., and Rechsteiner, M. (1982) Introduction of macromolecules into cultured mammalian cells by osmotic lysis of pinocytic vesicles. *Cell 29*, 33−41.
(18) Schafheutle, M. A., and Finkelmann, H. (1988) Shapes of micelles and molecular geometry: synthesis and studies on the phase behaviour, surface tension and rheology of rigid rodlike surfactants in aqueous solutions. *Liq. Cryst. 3*, 1369−1386.
(19) Riley, T., Govender, T., Stolnik, S., Xiong, C. D., Garnett, M. C., Illum, L., and Davis, S. S. (1999) Colloidal stability and drug incorporation aspects of micellar-like PLA-PEG nanoparticles. *Colloids Surf., B 16*, 147−159.
(20) Li, Y. P., Pei, Y. Y., Zhang, X. Y., Gu, Z. H., Zhou, Z. H., Yuan, W. F., Zhou, J. J., Zhu, J. H., and Gao, X. J. (2001) PEGylated PLGA nanoparticles as protein carriers: synthesis, preparation and biodistribution in rats. *J. Controlled Release 71*, 203-211.
(21) Kanaras, A. G., Kamounah, F. S., Schaumburg, K., Kiely, C. J., and Brust, M. (2002) Thioalkylated tetraethylene glycol: a new ligand for water soluble monolayer protected gold clusters. *Chem. Commun*. *20*, 2294−2295.
(22) Kriwet, B., Walter, E., and Kissel, T. (1998) Synthesis of bioadhesive poly(acrylic acid) nano- and microparticles using an inverse emulsion polymerization method for the entrapment of hydrophilic drug candidates. *J. Controlled Release 56*, 149−158.
(23) Karttunen, J., and Shastri, N. (1991) Measurements of ligand induced activation in single viable T-cells using the lacZ reporter gene. *Proc. Natl. Acad. Sci. U.S.A. 88*, 3972−3976.
(24) El-Shami, K., Tirosh, B., Bar-Haîm, E., Carmon, L., Vadai, E., Fridkin, M., Feldman, M., and Eisenbach, L. (1999) MHC class I-restricted epitope spreading in the context of tumor rejection following vaccination with a single immunodominant CTL epitope. *Eur. J. Immunol*. *29*, 3295−3301.
(25) Kim, T. S., Chung, S. W., and Hwang, S. Y. (2000) Augmentation of antitumor immunity by genetically engineered fibroblast cells to express both B7.1 and interleukin-7. *Vaccine 18*, 2886−2894.
(26) Diebold, S. S., Lehrmann, H., Kursa, M., Wagner, E., Cotten, M., and Zenke, M. (1999) Efficient gene delivery into human dendritic cells by adenovirus polyethylenimine and mannose polyethylenimine transfection. *Hum. Gene Ther. 10*, 775−786.
(27) Fukasawa, M., Shimizu, Y., Shikata, K., Nakata, M., Sakakibara, R., Yamamoto, N., Hatanaka, M., and Mizuochi, T. (1998) Liposome oligomannose-coated with neoglycolipid, a new candidate for a safe adjuvant for induction of $CD8^+$ cytotoxic T lymphocytes. *FEBS Lett. 441*, 353−356.
(28) Sparwasser, T., Koch, E., Vabulas, R. M., Heeg, K., Lipford, G. B., Ellwart, J. W., and Wagner, H. (1998) Bacterial DNA and immunostimulatory CpG oligonucleotides trigger maturation and activation of murine dendritic cells. *Eur. J. Immunol. 28*, 2045−2054.

BC049956F